# Fluidity of Sn-based eutectic solder alloys

**Carina Morando, Osvaldo Fornaro, Olga Garbellini & Hugo Palacio**

**Journal of Materials Science: Materials in Electronics**

ISSN 0957-4522
Volume 26
Number 12

J Mater Sci: Mater Electron (2015)
26:9478-9483
DOI 10.1007/s10854-015-3415-3

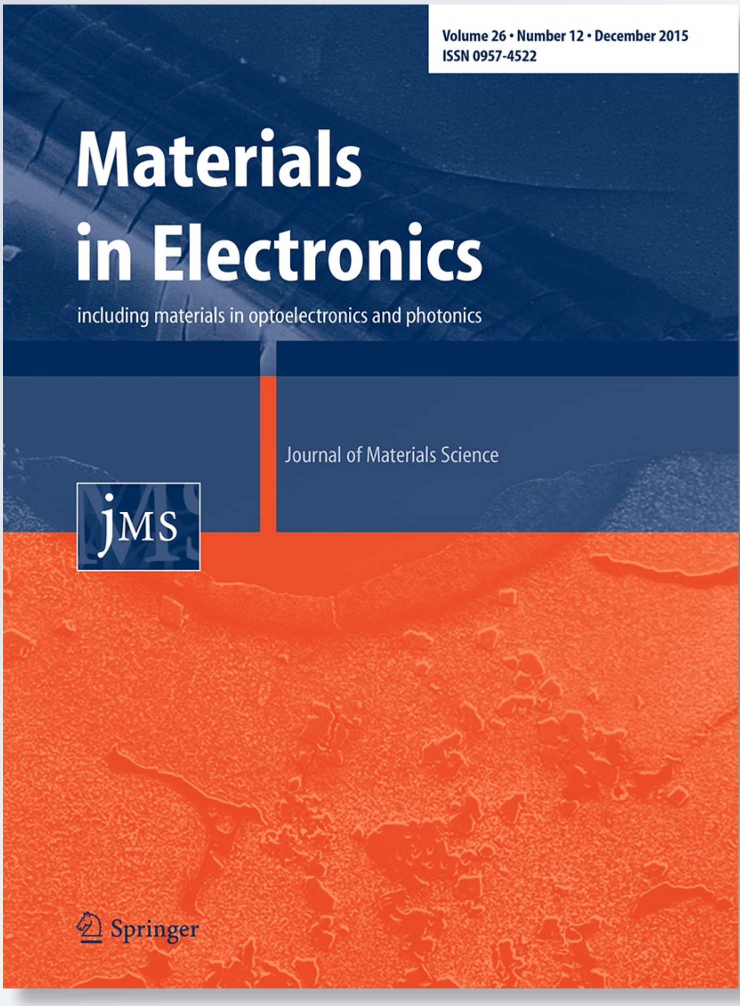


Springer

J Mater Sci: Mater Electron (2015) 26:9478–9483
DOI 10.1007/s10854-015-3415-3

# Fluidity of Sn-based eutectic solder alloys

Carina Morando[1,3] · Osvaldo Fornaro[1,3] · Olga Garbellini[2,3] · Hugo Palacio[2,3]

Received: 26 January 2015 / Accepted: 24 June 2015 / Published online: 9 July 2015


**Abstract** Eutectic alloys have a great importance in both academic and technological point of view. As regard technological applications such as casting, welding and joining, these systems offer lower melting point than the pure elements, and good fluidity. The fluidity length ($L_F$) is known as the distance travelled by the liquid metal forced to flow through a channel of small cross section, until it is stopped by solidification. Physical variables associated with the process are: metallostatic pressure, heat extraction rate at the metal-mold interface, overheating of the liquid metal and the physico-chemical properties of the metal or alloy (latent heat of fusion, density, viscosity, surface tension and solidification mode). In general, pure metals and alloys of eutectic composition have the highest values of fluidity, whilst intermediate composition alloys with greater solidification range show lesser fluidity lengths. Taking into account that the chemical composition plays an important role in the fluidity length by its relationship with the resulting microstructure, the aim of this work is to obtain fluidity values of binary and ternary lead-free metallic alloys in order to determine the relationships between the morphology and the fluidity length, and consequently, the influence on binary and ternary pro-eutectic alloys. Fluidity tests were carried out in a linear fluidity device, using lead-free Sn based alloys, extensively used for important industrial applications. The samples were characterized using optical microscopy, scanning electron microscopy and energy dispersive X-ray microanalysis. Usually, fluidity length ($L_F$) depends on solidification mode, latent heat of fusion of the alloy and the fluidity of the phases present in the microstructure.

✉ Carina Morando
carinamorando@yahoo.com.ar

1 Consejo Nacional de Investigaciones Científicas y Técnicas, Av. Rivadavia 1917 (C1033AAJ), Buenos Aires, Argentina

2 Comisión de Investigaciones Científicas de la Provincia de Buenos Aires, Av 526 e/10 y 11, B1906APP La Plata, Argentina

3 Centro de Investigación en Física e Ingeniería del Centro de la Provincia de Buenos Aires, (CIFICEN), Instituto de Física de Materiales Tandil (IFIMAT), Universidad Nacional del Centro de la Provincia de Buenos Aires, Pinto 399, B7000GHG Tandil, Argentina

## 1 Introduction

In the modern electronics industry, soldering is the most important technique to connecting the electronic devices and substrates. As a joining material, solder provides electrical contacts and facilitates thermal paths for heat dissipation, as well as mechanical integrity in electronic assemblies [1–3]. The eutectic Sn–Pb alloy is the most popular solder. In the last years the microelectronics industry has been moving away from Lead-containing solder alloys due to the harmful effects it has on environment and human health combined with the strict legislation (the so-called WEEE and RoHS directives) on banning the use of Lead-based solders [4, 5]. Simultaneously, there is a growing need for solders that can be used for applications with more demanding service conditions such as automotive or aerospace. For these purposes, Lead-free solder alloys (LFS) have been developed during the past decade to replace classic Sn–Pb eutectic solders [6]. A basic requirement for a candidate solder alloy to replace a Pb-containing solder is to have a specific freezing range compatible with existing equipment and components. Despite these reasons, the ideal solder alloy would be eutectic or near-eutectic, with a liquidus temperature low enough to avoid damaging the associated electronic components and a solidus temperature high enough to maintain joint reliability during thermomechanical fatigue. There are several LFS Sn-based alloys candidates such as Sn–Ag–Cu alloys (SAC alloys), containing Zn, In or Bi, which have attracted attention especially for automotive, industrial and electronic applications. Two of the main benefits of this system are its low melting temperature compared with the Sn–Ag binary eutectic alloy and its distinguished wetting behavior without losing strength. Also, the SAC solder-joint electrical properties seam to be attractive for both surface-mount and ball-grid-array assembly methods. Thus, Sn–Ag–Cu is considered one of the most favorable system as a Lead-Free standard alloy replacement [7].

Also, for technological applications such casting, welding and joining, this system offers lower melting point than the pure elements as so as a good fluidity, determined by the the fluidity length, $L_F$. This property is the distance travelled by a liquid metal forced to flow through a channel of small cross section until it is stopped by solidification. The $L_F$ is the resultant of the dynamic process taking place during the solidification into the vein. So, the measure length $L_F$ is not a physical property but a technological parameter that includes the interaction of a range of physical constants and also microstructure evolution during solidification [8]. The factors that affect the fluidity can be basically divided into (a) metallurgical variables such as composition, superheat, latent heat, surface tension, viscosity and mode of solidification (whether growth is planar, columnar or equiaxed) and (b) mold/casting variables such as part configuration, cooling rate, temperature, material and thr surface characteristics of the mold. Metallurgical factors are the inherent factors that influence the fluidity of each alloy system [9].

$$L_F = \frac{r\rho v(H + C_P(T - T_L))}{2h(T - T_{channel})} \quad (1)$$

This expression corresponds to a classically used simplified model developed by Flemings et al. [10] for planar front solidification in a cylindrical channel where heat flow is controlled through the interface metal-mold, $r$ is the radius of the channel, $\rho$ the density of the liquid, $v$ flow velocity, $H$ latent heat of fusion, $C_P$ the specific heat capacity, $T$ and $T_L$ the alloy and liquidus temperature of the alloy, $T_{channel}$ the temperature of the flow channel, and $h$ the heat transfer coefficient between the alloy and the flow channel. For given test variables ($r$, $v$, $h$, $T_{channel}$), $L_F$ increases with increasing initial melt superheat $(T - T_L)$, increasing specific heat capacity and increasing latent heat of fusion. Surface tension is not included in this equation, but it is known that influence $L_F$ when flow occurs in narrow channels, as it happens when solder alloys fill through-hole joints. Also, the alloy chemical composition plays a main role in the resultant fluidity length and has been extensively studied in the literature [10–12]. As it is well known, pure metals and alloys of eutectic composition have the highest values of fluidity, whilst intermediate composition alloys with greater solidification range show lesser fluidity lengths. This behavior is due to during the solidification of eutectic alloys the liquid transforms simultaneously into two solid phases, with zero or small freezing ranges that effectively eliminate the dendritic mushy zone thereby reducing segregation and shrinkage porosity while promoting excellent mold filling, avoiding the forming "in-situ" composites. In many other practical alloys that freeze dendritically, secondary phases are formed near the end of freezing by eutectic solidification [13].

When a liquid with eutectic composition solidifies, the resulting material generally consists of a dispersed two-phase microstructure that is approximately ten times finer than cells or dendrites of an intermediate composition growing under similar conditions. The exact arrangement of the two phases in the eutectic microstructures can vary widely, depending on the solidification conditions and the particular eutectic being solidified. Biloni and Boettinger [13] classified eutectic systems in two groups: regular and irregular. The criteria used for those authors are the entropy of fusion and the volume fraction of phases. If both phases have low entropy of fusion, it exhibits a regular or non faceted-non faceted morphology. If one phase has higher entropy than the other, the eutectic morphology results irregular or faceted-non faceted type. In a previous work thermal properties of this alloy family were extensively studied [14], including solidus and liquidus temperatures, solidification range and the amount of undercooling associated with the solidification using calorimetric techniques. These thermal properties are useful to interpret the solidification and the fluidity behavior of LFS alloys.

Based on the results obtained by the authors in previous works for AlCuSi system, [12, 15], the aim of this work is to analyze the fluidity of binary and ternary metallic alloys, close to the eutectic composition, in terms of solidification microstructure by means of linear fluidity tests corresponding to Pb free Sn based alloys extensively used for important industrial applications. The purpose was to determine the physical mechanism involved in experiments and the relationships between morphology of growth, microstructure and fluidity length, and consequently the influence on binary and ternary pro-eutectic alloys.

## 2 Experimental

### 2.1 Materials

Binary and ternary alloys were prepared in our laboratory by melting pure elements (purity 99.99 %) in an electric resistance-type furnace under inert Ar gas atmosphere, stirred for adequate homogenization and cast in stainless steel molds. The nominal compositions of the alloys are expressed as wt% of solute.

### 2.2 Fluidity tests

Fluidity Tests were carried out using a vacuum linear device similar to the developed by Ragone et al. [16] which is now widely used as a laboratory technique [12, 15]. The molten alloys were forced to flow into a channel of rectangular section under depress-casting, until it stops, and the $L_F$ distance into the channel was meassured. As the solidification microstructures depend on the cooling conditions, fluidity values were determined under two different cooling conditions: refractory sand mold giving a heat transfer coefficient at the metal-mold interface $hi = 0.2\,10^3\,\mathrm{J/m^2\,sK}$ (low cooling) and $hi = 5\,10^3\,\mathrm{J/m^2sK}$ (higher cooling) for Cu mold. In each experience the liquid alloy was forced to flow into the channel under constant metallostatic pressure $\Delta P =$ 2 or 15 mmHg for sand or Cu molds respectively to a casting temperature given by $T_C = T_L + \Delta T$ with $\Delta T = 20\,^{\circ}\mathrm{C}$. The mold was cooled in air. The sample was removed and longitudinally sectioned for metallographic observation. The represented data corresponds to the average of at least 5 experiments performed under the same experimental conditions. The dispersion range was 5 %.

### 2.3 Metallographic study

The solidified samples were polished for microstructural observations. Both Optical Microscopy (OM) and Scanning Electron Microscopy (SEM) were used to characterize the microstructure. Energy dispersive X-ray microanalysis (EDAX) was used to characterize the phase composition. Microstructural analysis was performed on metallographic specimens that were polished by means of standard metallographic procedures, etched with a solution of 0.5 ml of HF in $H_2O$ and followed by 2 % HCl in alcohol and electrolytically polished with butilcelosolve 80cc, 10cc glycerin and 10cc perchloric acid.

### 2.4 Thermal properties

As previously mentioned, thermal properties were determined by use of Computer-aided cooling curve analysis (CA-CCA) and Differential Scanning Calorimetry [14]. In this work, solidus and liquidus temperatures were determined to stablish the experimental conditions of fluidity tests. Also latent heat of fusion was determined for each alloy. Cooling curves were carried out using small samples between 50 and 80 g in an electric furnace, electronically controlled. Chamber and sample temperatures were taken by using K type thermocouples wired to a NI-USB 9211 acquisition data interface, connected to a personal computer. The latent heat of fusion ($H_F$) was determined using a scanning calorimeter Heat Flux DSC Rheometric Scientific SP, with a line stability better than 1 mW in the measurement range used. The samples used are 6 mm in diameter and 20 mg of weight. The curves were obtained for scan rates of 5 and 10 K/min.

## 3 Results and discussion

Table 1 contains the nominal composition of the Sn based alloys expressed as wt% of solute, Fluidity Length obtained for the two cooling conditions: slow cooling (refractory sand mold) $L_{FS}$ and fast cooling (Cu mold) $L_{FF}$, Latent Heat of fusion ($H_F$), constituent phases (according to the microstructures analysis by EDAX) and the melting temperature ($T_M$) experimentally determined.

Figure 1 is a summary of the cooling curves obtained for different eutectic Sn based alloys, pure Sn and Sn–Pb eutectic studied under controlled conditions [14]. We can observe the typical aspect of Temperature-time curve, characteristic of the solidification process, where particularly we need the solidification temperature to define the $T_C$. These data are summarized in the last column of Table 1. The temperature $T_M$ and enthalpy of melting were obtained using differential scanning calorimetry, as can be seen in Fig. 2 [14].

The observed fluidity behavior was similar for both cooling rates. The results for the refractory sand mold ($L_{FS}$) were similar to those obtained for the Cu mold ($L_{FF}$). These

**Table 1** Composition, constituent phases, fluidity length ($L_F$), latent heat of fusion ($H_F$) and fusion temperature ($T_M$) of the Sn based alloys

| Alloy | Composition | Constituent phases | $L_{FS}$ (cm) | $L_{FF}$(cm) | $H_F$ (J/g) | $T_L$ (°C) |
|---|---|---|---|---|---|---|
| #1:Sn | Sn | | 20.8 | 21.5 | 53.85 | 230.1 |
| #6:SnPb | Sn–37%Pb | Sn + PbSn | 15 | 17.6 | 42.4 | 177.7 |
| #3:SnAg | Sn–3.5%Ag | Sn + $Ag_3Sn$ | 12.5 | 13.9 | 56.07 | 218.3 |
| #2:SnCu | Sn–0.7%Cu | Sn + $Cu_6Sn_5$ | 11.8 | 13.5 | 56.28 | 224.5 |
| #5:SnZn | Sn–9%Zn | Sn + ZnSn | 14 | 16.4 | 56.2 | 196.9 |
| #7:SnBi | Sn–57%Bi | Bi + SnBi | 20.5 | 21.5 | 52.1 | 134.7 |

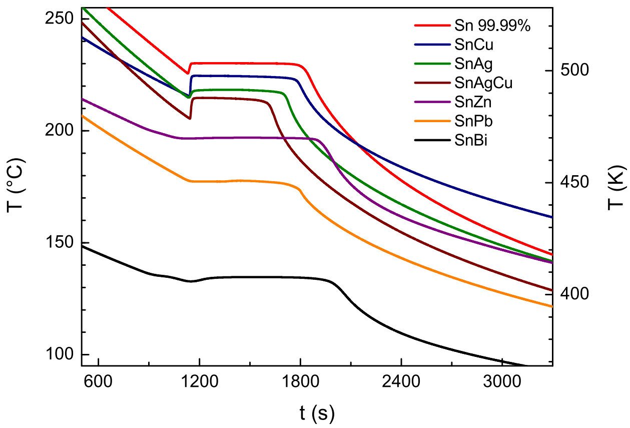


**Fig. 1** Temperature–time cooling curves obtained for Sn-based eutectic alloys and pure Sn

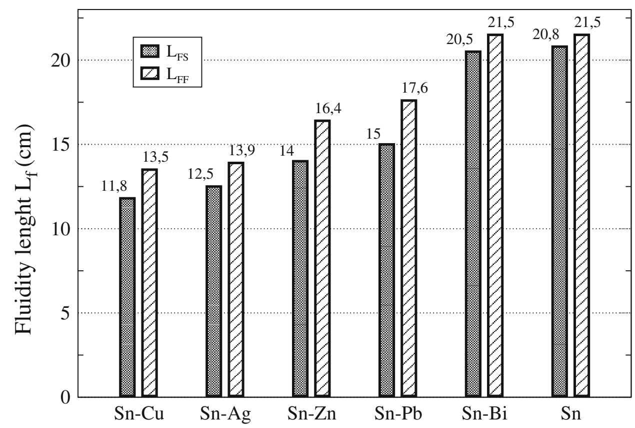


**Fig. 3** Fluidity length measured for both solidification conditions for LFS alloys, eutectic SnPb and pure Sn

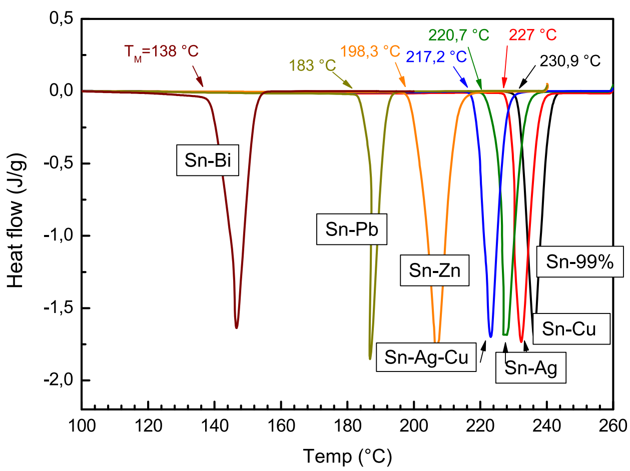


**Fig. 2** Calorimetric DSC curves corresponding to the melting of Sn solder family alloys obtained at $\alpha = 10\,°C/min$

results can be observed in Fig. 3. In general, an increase of the $L_F$ is observed in the experiences made in the sand mold due to the slower heat extraction. It is possible to note that the greater differences are given at the alloys with less $L_F$, close to 15 % for Sn–3.5%Ag, Sn–0.7%Cu, Sn–37%Pb and Sn9%Zn eutectic alloys, whilst for pure Sn as for Sn57%Bi, the difference for both conditions was approximately 4 %. To interpret these results, is necessary to analyze the microstructure obtained in each case.

Figure 4 shows Optical Micrographs (OM) of Sn–37%Pb eutectic alloy under different cooling conditions: (a) fast cooling (Cu mold) and (b) slow cooling (refractory sand mold). The microstructure consists on a mixture of fine Sn-rich (light regions) and Pb-rich (dark area) solid solutions forming a lamellar regular eutectic microstructure. The cooling rate affect significantly the microstructures of the solder alloys. Ochoa et al. [17] showed that an increase in solidification speed produces a refinement in the microstructure (Sn dendrites decrease in size). This is consistent with Fleming's solidification theory, which proposed that rapid solidification decreases the time needed for diffusion resulting in a finer dendritic microstructure [10]. Figure 5 exhibit OM of the microstructure of a) Sn–3.5%Ag and b) Sn–0.7%Cu binary eutectic alloys. The

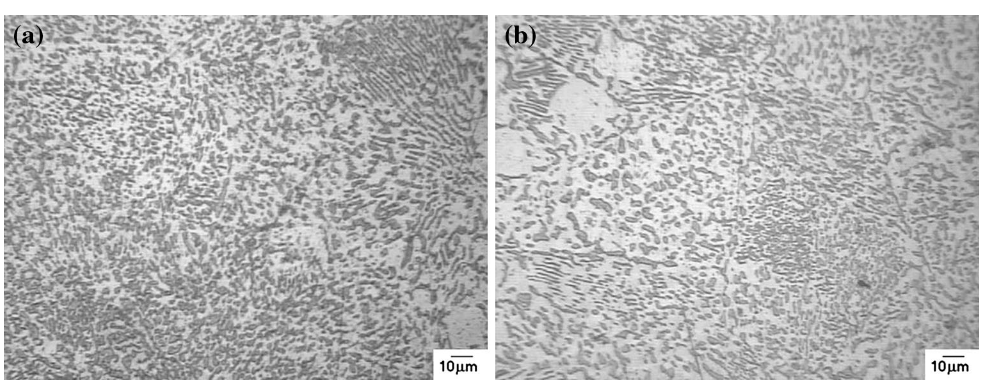


**Fig. 4** Optical micrographs of the Sn–37%Pb eutectic alloy, **a** Cu and **b** refractory sand mold, at the same magnification for microstructure refinement comparison

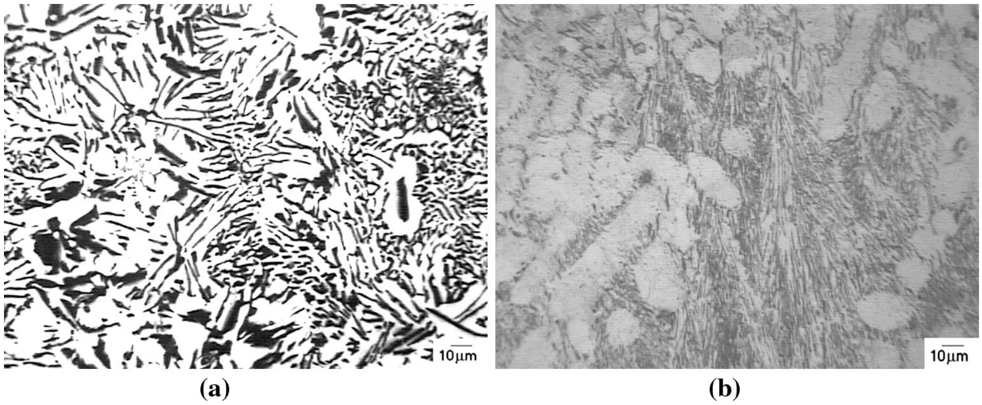


**Fig. 5** Optical micrographs of the **a** Sn–3.5%Ag and **b** Sn–0.7%Cu eutectic alloys

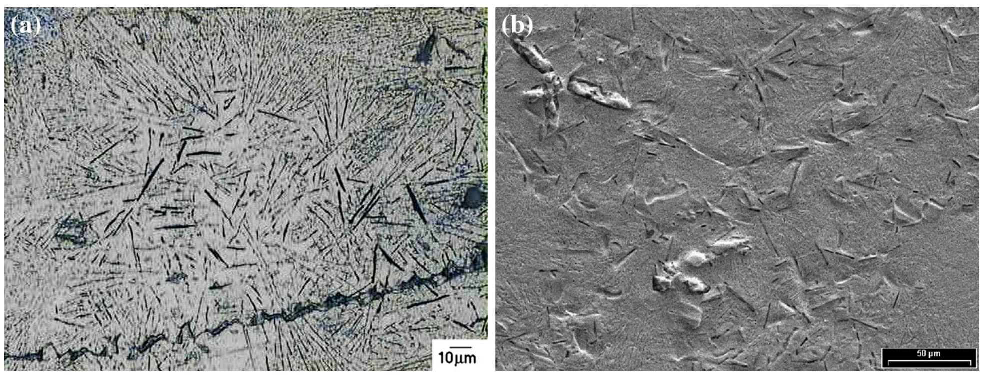


**Fig. 6** **a** Optical and **b** scanning electron micrographs of the Sn–9%Zn eutectic alloy

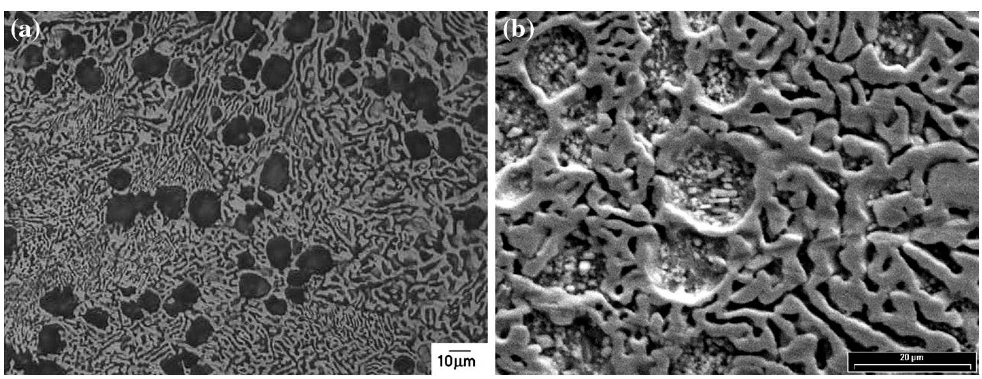


**Fig. 7** **a** Optical and **b** scanning electron micrographs of the Sn–57%Bi eutectic alloy

binary eutectic microstructure either in Sn–3.5%Ag or Sn–0.7%Cu is a mixture of the intermetallic particles, $Ag_3Sn$ or $Cu_6Sn_5$, in the $\beta$-Sn matrix. It consists of two regions, the hite region (primary Sn phase) surrounded by a dark network. These alloys exhibit a faceted-non faceted morphology corresponding to irregular eutectics, where the non-faceted phase is Sn and the faceted phase is $Ag_3Sn$ or $Cu_6Sn_5$, respectively. Figure 6 shows (a) OM and (b) Scanning Electron Micrographs (SEM) of Sn–9%Zn binary eutectic alloy. The structure corresponds to irregular eutectic, it is formed by a Sn-rich matrix and Sn–Zn needles, as can be seen in the micrographs. The constituent phases are marked on the SEM micrograph and were determined by EDAX. Figure 7 shows (a) OM and (b) SEM micrographs, the typical microstructure of Sn–57%Bi binary eutectic alloy. It is a regular globular kind of structure, that consists of a mixture of Bi-rich crystals in an eutectic matrix composed by Sn (light phase) and Bi (dark phase).

In general, the lamellar regular eutectic like Sn–37%Pb. Sn–3.5% Ag and Sn–0.7% Cu eutectic alloys have the lowest fluidity values of the Sn based alloys analyzed. As it was mentioned above, both have a similar structure, with eutectic formation around the primary phase. The fluidity of Sn–9% Zn is greater, their morphology is irregular or non-faceted faceted type as in the case of Sn–3.5% Ag and Sn–0.7% Cu, although in this case it has an high percentage of eutectic phase, which could explain the higher fluidity. Sn–37% Pb and Sn–57%Bi binary alloys have a lamellar eutectic microstructure corresponding to a regular type eutectic and have a greater fluidity than the one of irregular eutectics. These results agree with those obtained in previous works for other eutectic systems by Garbellini et al. [12, 15] and Di Sabatino [18]. The Sn–Pb and Sn–Bi phase diagrams are relatively symmetrical binary eutectic systems causing the eutectic mixtures to solidify as lamellar of similar volume fractions of two simple metal phases.

## 4 Conclusions

In this work the fluidity of Pb free Sn based eutectic alloys was studied. The results were related to resultant microstructures: Fluidity Length values obtained for the refractory sand mold (slow cooling) were similar to those obtained for the Cu mold (fast cooling). The cooling rate affects significantly the microstructure of the alloys, resulting in the refinement of the microstructure and finer dendrites morphology. This is a consequence of the increment in the solidification velocity, decreasing the time needed for diffusion. Regular or non faceted-non faceted binary eutectics alloys the fluid flow better than irregular or non faceted-faceted eutectics, due to the solidification mode. In the first group, liquid-solid interface is planar for each phase, as in pure metals whilst the second group shows an irregular morphology. formed by a primary dendritic phase surrounding faceted intermetallic phases. Analysis of the solidification microstructures of the samples permits the correlation of Fluidity Length with the solidification mode, latent heat of fusion of the alloy and the fluidity of the phases present in the microstructure.

**Acknowledgments** This work was carried out at CIFICEN (Centro de Investigaciones en Física e Ingeniería del Centro de la Provincia de Buenos Aires, CONICET-UNCBA) and IFIMAT (Instituto de Física de Materiales Tandil, UNCPBA-CICPBA-MT) and has been partially supported by ANPCyT (Agencia Nacional de Promoción Científica y Tecnológica, CONICET (Consejo Nacional de Investigaciones Científicas y Técnicas), SeCAT-UNCPBA (Secretaría de Ciencia, Arte y Tecnología de la Universidad Nacional del Centro de la Provincia de Buenos Aires) and CICPBA (Comisión de Investigaciones Científicas de la Provincia de Buenos Aires).

## References

1. M.M. Schwartz, S. Aircraft, *Welding, Brazing, and Soldering*, volume 6 of *ASM Metals Handbook*. ASM Intl. pp. 126–129 (1993)
2. R. Wassink, *Soldering in Electronics*, 2nd edn. (Electrochemical Publications Ltd, Ayr, 1989)
3. R. Strauss, *Surface Mount Technology* (Butterworth-Heinemann, Oxford, 1994)
4. Directive 2002/95/EC on the restriction of the use of certain hazardous substances in electrical and electronic equipment. European Parliament and the Council of 27 January 2003 (OJ L 37, 13.2.2003, p. 19)
5. Directive 2002/96/EC on waste electrical and electronic equipment. European Parliament and the Council of 27 January 2003 (OJ L 37, 13.2.2003, p. 24)
6. P. Lauro, S. Kang, W. Choi, D.-Y. Shih, J. Electron. Mater. **32**, 1432–1440 (2003)
7. S.-H. Huh, K.-S. Kim, K. Suganuma, Mater. Trans. JIM **42**, 739–744 (2001)
8. C. Gourlay, J. Read, K. Nogita, A. Dahle, J. Electron. Mater. **37**, 51–60 (2008)
9. K. Ravi, R. Pillai, K. Amaranathan, B. Pai, M. Chakraborty, J. Alloys Compd. **456**, 201–210 (2008)
10. M.C. Flemings, *Solidification Processing* (McGraw Hill, New York, 1974)
11. J. Campbell, Cast Metals **4**, 101–102 (1991)
12. O.B. Garbellini, H.A. Palacio, H. Biloni, Cast Metals **3**, 82–89 (1990)
13. H. Biloni, W.J. Boettinger, in *Solidification, volume II of Physical Metallurgy*, 4th edn., ed. by R.W. Cahn, P. Haasen (Elsevier Science Publishers, Amsterdam, 1996), pp. 669–842
14. C.N. Morando, O. Fornaro, O.B. Garbellini, H.A. Palacio, J. Mater. Sci. Mater. Electron. **25**, 3440–3447 (2014)
15. O. Garbellini, C. Morando, H. Palacio, H. Biloni, Int. J. Cast Metals Res. **17**, 12–16 (2004)
16. D.V. Ragone, C.M. Adams, Trans. Am. Foundrym. Soc. **64**, 640–648 (1956)
17. F. Ochoa, J. Williams, N. Chawla, J. Electron. Mater. **32**, 1414–1420 (2003)
18. M.D. Sabatino, F. Syvertsen, L. Arnberg, A. Nordmark, Int. J. Cast Metals Res. **18**, 59–62 (2005)